Influence of buckling parameter on load bearing deterioration of steel bridge piers during long duration time motions

T. Kitahara & Y. Ohtani

Kanto Gakuin University, Yokohama City, Kanagawa, Japan.

Y. Kishi

Tokyo Metropolitan University, Hachioji City, Tokyo, Japan.

T. Yamaguchi

Osaka City University, Osaka City, Osaka, Japan.

ABSTRACT: Recently, the occurrence of long duration time seismic motion is predicted during huge trench-type earthquakes around Japan, and dozens of cyclic behaviors are focused as the external force to cause serious damage to structures. However, the seismic performance of steel bridge piers subjected to such a wave has not been investigated sufficiently. Furthermore, local buckling affects the load carrying capacity of steel bridge piers under the dozens of cyclic motions. Hence, in this study, the load capacity of steel bridge piers was evaluated in the elastic range after maximum yield displacement with cyclic loading. Finite element analysis conducted to confirm the effect of width–thickness ratio on buckling parameter. The numerical analysis results suggest that the load-carrying capacity during cyclic loading decreases with decreasing width–thickness ratio parameter.

1 INTRODUCTION

After the 1995 Southern Hyogo Prefecture Earthquake, it was recognized to consider the strength and deformation performance in the plastic zone for the seismic design code, especially for many single pillar-type piers widely used as the city viaduct. The evaluation of the seismic performance of such steel piers was carried out after the earthquake damage (Usami et al. 1996). In addition, for the establishment of the seismic design method, the strength and deformation performance was quantitatively evaluated based on the results of static loading and cyclic loading tests (Aoki et al. 2005). However, the cyclic loading tests were repeated within 3 times for each load level.

On the other hand, when the huge oceanic trench-type earthquake occurs, long duration time motion is observed. In fact, the Great East Japan Earthquake in 2011 lasted for more than three minutes, and it has been noted as the factor that affected the response of the structures.

Long duration time motion is predicted during huge trench-type earthquakes at Nankai trough in Japan, and dozens of cyclic motions were focused on the external forces to cause serious damage to the structures. However, the performance of steel bridge piers subjected to long duration time motion has not been investigated sufficiently.

Static and cyclic loading tests were carried out to examine the load-bearing capacity of steel that is widely used in piers of elevated bridges in urban areas when they are subjected to long-duration seismic forces in the previous study (Kitahara et al. 2010). Consequently, it was found that the load bearing capacity after maximum load decreased about 10% owing to local buckling at cyclic loading of more than 10 times. However, the structural characteristics of the numerical model were designed based on the old specification. Hence, width–thickness ratio parameter was larger than that presently accepted.

The width–thickness ratio parameter (= R_f) of the plates in structural steel members influences on local buckling. Thus, it is necessary to evaluate the influence of width–thickness ratio parameter for decreasing the load bearing capacity of steel bridge piers during the long duration time motions. In this study, finite element analysis was used to verify the load bearing deterioration of steel bridge piers during long duration time motions.

2 NUMERICAL ANALYSIS

In this study, the difference of the width–thickness ratio parameter in reducing the strength of locally buckled steel bridge piers was examined. Numerical analysis was carried out considering material and geometrical nonlinearities. As the structural characteristics of the FEM models, three different width-thickness ratio parameters were considered based on actual data from steel bridge piers.

2.1 Numerical modeling

Numerical models have stiffened box-shaped cross sections which based on the single pillar-type piers widely used in city viaducts. In order to follow the response of the stiffener plate constituting in detail, finite element analysis was applied. Then, commercial software DIANA 9.4.4 (TNO DIANA) was used in this study.

According to the analysis results of the past, it is found that the upper side of the piers behave elastically within the boundary conditions. Therefore analysis models are simplified to minimize the calculation time, using isoparametric curved surface shell element up to a height of about 1/3 from the base to the pier and a beam element about 2/3 from the top as shown in Figure 1. Furthermore, the FE models were 1/2 vertical partial models considering the symmetry of the pier's cross-section and loading conditions.

Figure 1. Numerical model. (R_f = 0.66)

2.2 Buckling parameter

Values of buckling parameters are critical to estimate the load carrying capacity of steel bridge piers. In the seismic design of the box-section steel piers, the values of slenderness and width–thickness ratios are constrained to prevent buckling failure. These parameters are calculated by the following equations:

$$R_f = \frac{1}{\pi}\sqrt{\frac{12\left(1-v^2\right)}{k}\cdot\frac{\sigma_y}{E}}\left(\frac{b}{t}\right) \tag{1}$$

$$\bar{\lambda} = \frac{1}{\pi}\sqrt{\frac{\sigma_y}{E}}\left(\frac{l}{r}\right) \tag{2}$$

where, R_f is the width–thickness ratio parameter, v is Poisson's ratio, k is the buckling coefficient of the stiffener plate (=$4n^2$), n is the number of subpanels in each plate, σ_y is the yield stress, E is Young's

modulus, b is the plate width, t is the plate thickness, $\bar{\lambda}$ is the slenderness ratio parameter, l is the effective buckling length, and r is the radius of gyration.

Structural characteristics of analysis models such as cross sections were determined based on existing steel piers and test specimens from previous researches (Suzuki and Usami 1995, Yoshizaki et al. 1999). Since the numerical models were referring to existing piers that were designed with the old code, the cross-sectional shapes were not uniform. For the same reason, width–thickness ratio parameters that did not conform to the current design code were also targeted (Japan Road Association 2003). Figure 2 and Table 1 show the model cross-sections and specifications.
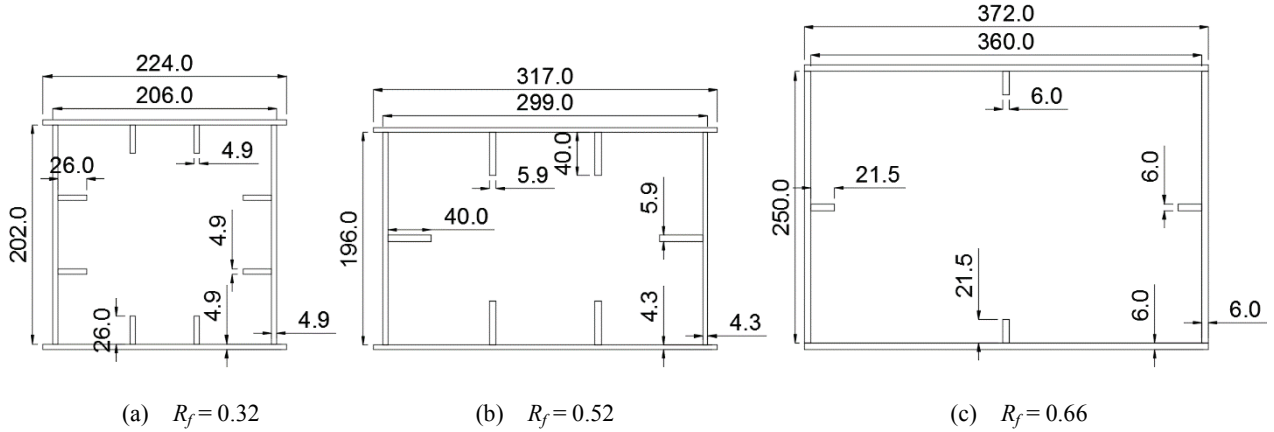

(a) $R_f = 0.32$ (b) $R_f = 0.52$ (c) $R_f = 0.66$

Figure 2. Cross-sections of numerical models. (unit: mm)

Table 1. Specifications of numerical models.

Width-Thickness Ratio: R_f		0.32	0.52	0.66
Slenderness Ratio: $\bar{\lambda}$			0.37	
Height of Piers	[mm]	1190	1192	1572
Width of Flange	[mm]	224	317	372
Width of Web	[mm]	202	196	250
Thickness of Plate	[mm]	4.9	4.27	6.0
Width of Rib	[mm]	26	40	21.5
Thickness of Rib	[mm]	4.9	5.91	6.0
Cross-Section Area	[mm^2]	5194	5799	7980
Moment of Inertia	[mm^4]	3426×10^4	3839×10^4	9215×10^4
Elastic Modulus: E_1	[N/mm^2]		2.06×10^5	
Secondary Elastic Modulus: E_2	[N/mm^2]		E_1/100	
Axial Force	[kN]	171.4	191.4	263.3
Axial Force Ratio: P/P_y		0.1	0.1	0.1
Yield Displacement: δ_y	[mm]	7.14	7.41	10.07
Yield Bending Moment: M_y	[N・mm]	873.5×10^5	1066×10^5	2321×10^5
Number of Element Mesh	Height	30	30	40
	Flange Width	19	19	26
	Web Width	34	24	38
	Vertical Rib	5	4	2
	Diaphragm	6	7	8

3

2.3 Material and geometrical non-linearity

Young's modulus and yield values were assumed based on the results of coupon tests from previous studies. Bi-linear kinematic hardening was assumed for the stress–strain relation as shown in Figure 3 and the von Mises yield criterion was used. The secondary stiffness of the bi-linear model was defined as 1/100 of the initial stiffness. The geometrical non-linearity in the numerical calculation was formulated by the total Lagrangian method. The Newton–Raphson method was used in the convergence calculations.
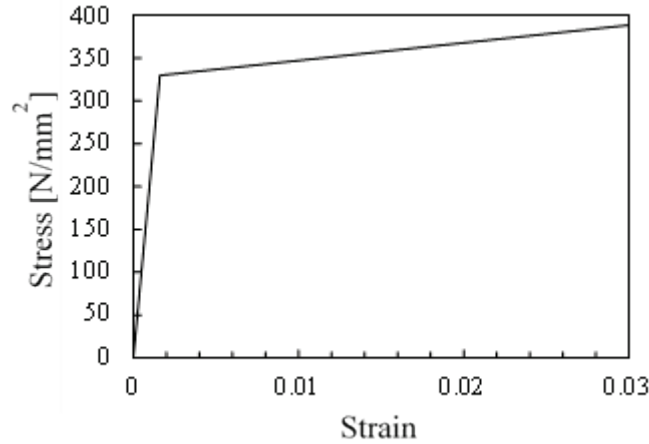

Figure 3. Stress–strain relation.

2.4 Initial imperfection

Numerical models considered the initial deflection of the pier base using a curved shell element to the first stage diaphragm. The second stage or higher diaphragms and beam elements were not considered. The initial global deflection W_g and the local deflection W_L are defined by equations (3) and (4), respectively (Kitada et al. 1994),

$$W_g = W_1 \cdot \sin \frac{\pi x}{a} \cdot \sin \frac{\pi y}{b} \tag{3}$$

$$W_L = W_2 \cdot \sin \frac{n\pi x}{a} \cdot \sin \frac{n\pi y}{b} \tag{4}$$

where, a is the diaphragm interval, b is the width of stiffener plate, n is the number of divisions of the stiffener plate, W_1 is the maximum vertical distance of global system, and W_2 is the maximum vertical distance of local system. In addition, tolerance W_1 is the $a/1000$, W_2 is $(b/n)/150$.

Generally, it is necessary to define the residual stress for the ultimate strength calculation of steel structural members, however, it was not considered in this study. As the reason of this definition, this study focused on the behavior of steel bridge piers in a domain of cyclic loading after the maximum load in the plastic region.

2.5 Boundary conditions and loading pattern

The six degrees of freedom in the direction of translation and rotation were fixed at the base. The axial force was equivalent to the dead load of the superstructure on the piers, and the axial force determined the initial stress state. The horizontal displacement of the top of the pier model under the axial force loading and the local buckling at the pier base were calculated.

Horizontal loading was combined gradual and a repeat type displacement such as shown in Figure 4. Dozens of cyclic displacement motions were observed during huge ocean-trench type earthquakes, and many components of the ground motions cannot influence on the structural behavior in plastic range because of the small displacements. Therefore, cyclic ground motions were replaced by cyclic displacements as load pattern in the analysis. In addition, the amplitudes of the cyclic displacements in

the analysis were set at $1.4\delta_y$, $1.6\delta_y$, and $1.8\delta_y$ ($\leq 2.0\delta_y$), based on Timoshenko's beam theory to constrain the behavior in the plastic range.

The loading patterns in each model were defined by pushover analysis. Elastic range cyclic loading was assumed for a long duration vibration which continues hundreds of seconds after the main tremor of the long ground motion.
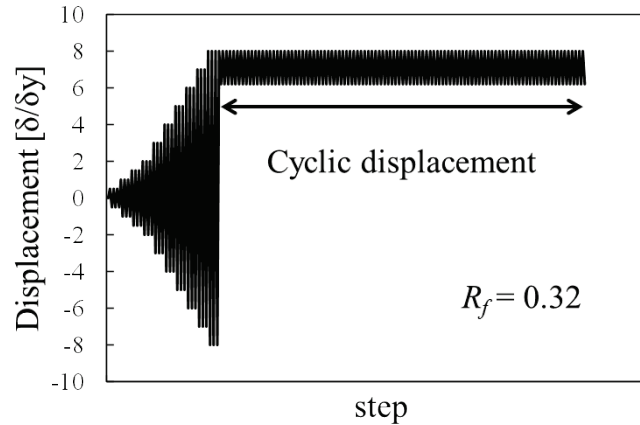

Figure 4. Loading pattern.

3 WIDTH-THICKNESS RATIO AND LOAD BEARING DETERIORATION

Figure 5 shows the load–displacement relation for each finite element model. The vertical and horizontal axes are dimensionless; they are defined by the horizontal yield load H_y and the horizontal yield displacement δ_y, respectively. Comparing the envelopes of the three numerical models, the loads of the model with R_f of 0.52 and 0.66 are greatly reduced. These results show that the width-thickness ratio parameters of the stiffened plate affects the behavior after the maximum load.
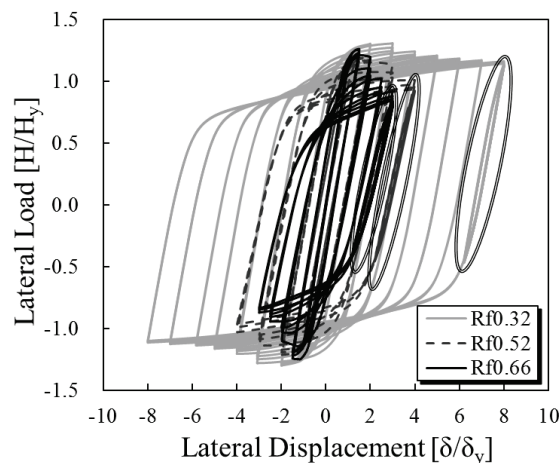

Figure 5. Load–displacement relation at $1.8\delta_y$.

Figure 6 shows the load–displacement relation for cyclic displacement less than $2.0\delta_y$. The area is marked by the circle in Figure 5. Although the results for the cases of small amplitudes are close to the linear hysteresis, every response hysteresis shows non-linearity. Thus, even though the load amplitude in the elastic range after the maximum load decreases, the steel piers behave plastically. Figure 6 (c) shows a partial enlarged view of the load decrease at constant displacement level in every cyclic loading. To confirm the correlation between the width-thickness ratio parameter and the strength reduction, the load bearing deterioration is shown as below.

Figure 7 shows the degraded strength for the different width–thickness ratio parameters. Generally, the strength reduction for small R_f models converges after a small number of cycles. In contrast, for large

R_f, there is convergence after 100 iterations. These results show that the load bearing deterioration of thinner-walled pier sections increces with the progress of local buckling.

Strength reduction increases with increasing cyclic amplitude. In particular, degradation is 20 times higher than the initial for R_f = 0.66. These results show that the cyclic amplitude influences the strength deterioration of steel bridge piers at an early stage after the maximum load.
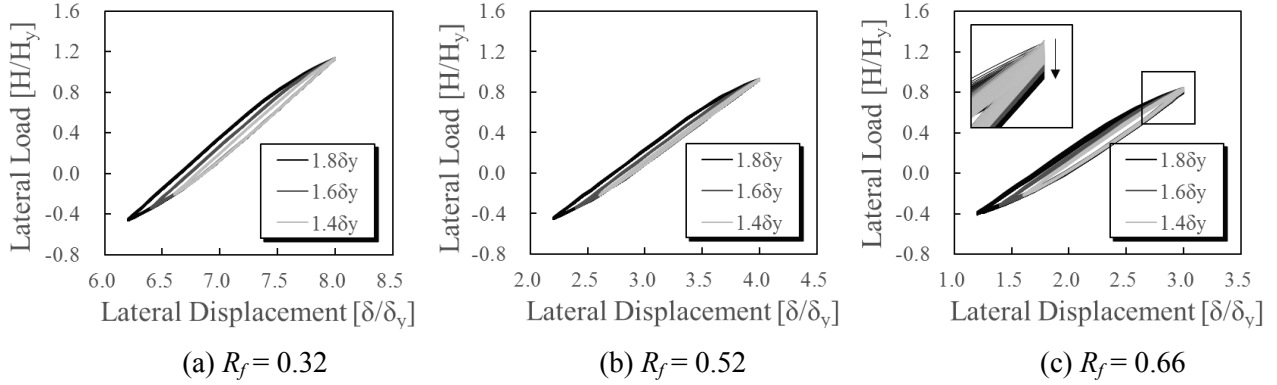

(a) R_f = 0.32   (b) R_f = 0.52   (c) R_f = 0.66

Figure 6. Load–displacement relation. (enlarged view of cyclic part)

(a) $1.4\delta_y$ (b) $1.6\delta_y$ (c) $1.8\delta_y$
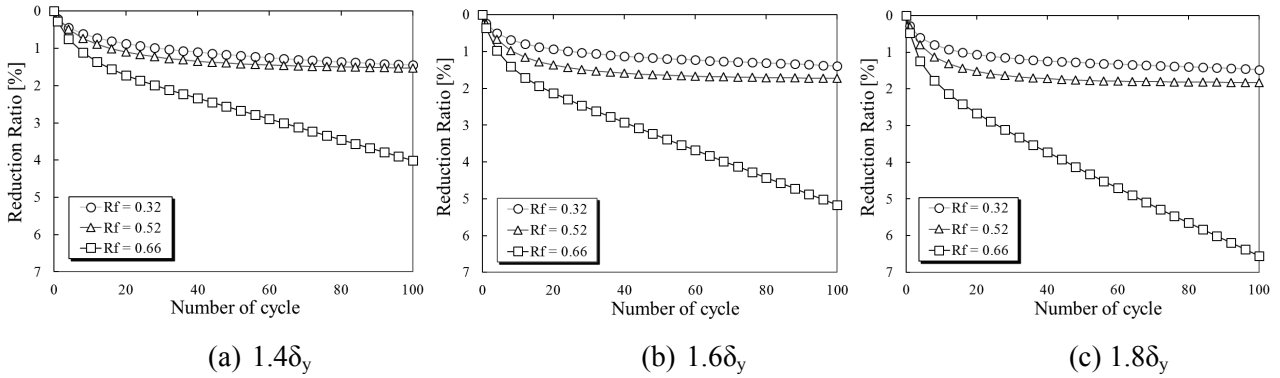
Figure 7. Strength reduction ratio.

4 CONCLUSION

In this study, the influence of buckling parameters on the load bearing deterioration of steel bridge piers subject to long duration time motions was verified by numerical calculations. Moreover, the behavior of steel bridge piers that were affected by cyclic loading after the maximum load is calculated by finite element method. The results of this study are summarized as follows.

1) The width–thickness ratio parameter of steel bridge piers greatly influences on the behavior of the load-displacement hysteresis envelope.

2) Horizontal displacement of less than $2.0\delta_y$ in Timoshenko's beam theory was applied to the top of the models and cyclic loading after the maximum load. Nonlinear behavior was observed in every case with the progress of local buckling and the load bearing capacity decreased after local buckling occured.

3) The thinner the plate thickness is (large R_f), the grater the strength reduction is with the progress of local buckling. Furthermore, the influence of cyclic motion on the strength deterioration is greater than the cross-section consisted of thicker stiffened plates.

Besides local buckling, the behavior of the material also decreases strength because of the reduction in the yield surface due to cyclic loading. Hence, authors use a modified two surface model as a constitutive law to properly reproduce the cyclic elasto-plastic behavior of steel materials.

REFERENCES:

Japan Road Association. 2003. Specifications for Highway Bridges: Part V, Seismic Design ver2002. Maru-zen.

Kazuya Yoshizaki, Tsutomu Usami, Daisuke Honma 1999. Pseudodynamic tests of steel bridge piers with purpose of reducing residual displacements. *Journal of structural engineering*. Vol.45A. 1017-1026. (in Japanese)

Moriaki Suzuki, Tsutomu Usami 1995. Estimating formulas of strength and deformation capacity of steel bridge pier model under cyclic loading. *Proceedings of JSCE*. No.519. 115-125. (in Japanese)

Takeshi Kitahara, Kentaro Tanaka, Takashi Yamaguchi 2010. Load Bearing Capacities of Steel Bridge Piers Subjected to Long-duration Time Motions. *Proceedings of 9th US national and 10th Canadian Conference on Earthquake Engineering*, Toronto, Canada. CD-ROM Proceedings No.843.

Tetsuhiko Aoki, K.A.S.Susantha 2005. Seismic Performance of Rectangular-Shaped Steel Piers under Cyclic Loading. *Journal of structural engineering*. ASCE. Vol.131 Issue 2, 240-249.

Toshiyuki Kitada, Hiroshi Nakai, Masashi Kunihiro, Naoki Harada 1994. Study on interaction curve for ultimate strength of unstiffened thin-walled box cross sections subjected to compression and bending. *Journal of structural engineering*. Vol.40A. 331-342. (in Japanese)

Tsutomu Usami, Satish Kumar 1996. Damage evaluation in steel box columns by pseudodynamic tests. *Journal of structural engineering*. ASCE. Vol.122 Issue 6. 635-642.